Polar
Geophysical
Institute

PRACTICE OF CCD CAMERAS' CALIBRATION BY LED LOW-LIGHT SOURCE

B.V. Kozelov[1], B.U.E.Brändström[2], F. Sigernes[3], A.V. Roldugin[1], S.A. Chernouss[1]

[1]*Polar Geophysical Institute, Apatity Murmansk region, 184209 Russia*
[2]*Swedish Institute of Space Physics, Kiruna, Sweden*
[3]*The Kjell Henriksen Observatory, UNIS, Longyearbyen, Norway*

Abstract. Two identical CCD cameras used for auroral observations (*Kozelov et al.*, 2012) have been calibrated by LED low-light source PGI-Chernouss-38AM. The calibration factor as a function of the wavelength and the camera gain was deduced. Previously the light source PGI-Chernouss-38AM (SID 105) was absolutely calibrated during the intercalibrational workshop of optical low light sources (*Brändströmet al.*, 2012), and it was found some issues motivated additional studies of the light source. The current-voltage and emission intensity characteristics of the light source have been measured. It have been found recommendation for the light source users: i) the current value should be measured; ii) the light source should be equipped by external stabilized electric power source; iii) the setting "3" of the lamp and region of wavelengths < 500 nm should be avoided due to peaked spectrum.

1. Introduction

The Multiscale Aurora Imaging Network (MAIN) system contains 4 cameras located near Apatity, Kola Peninsula, Russia (*Kozelov et al.*, 2012). Two of these cameras are identical, they are based onAVT Guppy F-044B NIR (1/2"CCD) digital cameras with Fujinon HF25HA-1B (1:1.4/25mm) lens and additionally equipped by glass filter on blue-green region.These cameras are using as a stereoscopic pair for measurements of altitude of auroral luminosity. Comparison of the altitude with results of numerical models can give us an important geophysical characteristic – the energy of electrons precipitated to the ionosphere and excited the aurora. Knowledge of absolute intensity of auroral emission can be used to deduce the second characteristics - the energy flux of precipitated electron. More details about geophysical application of the camera system were presented in (*Kozelov et al.*, 2012). Each auroral camera contains of not only the CCD camera, but lens, optical filter(s) and income window of camera dome, therefore this rather complicated optical system as a whole is a subject of special absolutely calibration. The "black" (dark current) and "white" fields needed to compensate the CCD sensor inhomogeneity are also usually measured during calibration.

The absolute calibration of light intensity observed by CCD camera can be formally described by the expression:

$$J(x,y) = [C_{obs}(x,y) - C_{BF}(x,y)] \left\{ \frac{C_{WF}(x_0,y_0) - C_{BF}(x_0,y_0)}{C_{WF}(x,y) - C_{BF}(x,y)} \right\} K_\lambda \quad (1)$$

Here: (x,y) are the pixel coordinates (column and line numbers) in CCD matrix,$C_{obs}(x,y)$ [CTS s^{-1}] is the raw count rates in the CCD pixels,$C_{BF}(x,y)$ and $C_{WF}(x,y)$ are "black" and "white" fields,$C_{BF}(x_0,y_0)$ and $C_{WF}(x_0,y_0)$ are average values of count rates in calibration region of "black" and "white" fields,K_λ[R s CTS^{-1}] is a calibration factor. Here we use traditional units for aurora light intensity 1 Rayleighs = 10^6 photons cm^{-2} s^{-1}.

The quantity inthe curly braces of (1)wewill refer as $Q(x,y)$. This matrix characterizes the relative inhomogeneity of the CCD response due to given optical system and individual features of the CCD pixels.

In common case for CCD cameras all quantities should be dependent on gain control, and in our case

$$K_\lambda = F_\lambda \exp(-k_\lambda g), \quad (2)$$

where$g$ is the camera gain level, F_λ and $k_\lambda$are camera-type-dependent constants, which should be obtained during calibration by test source.So, we need to measure the following quantities: F_λ, k_λ, $Q(x,y, g)$ and$C_{BF}(x,y, g)$.

First two constants have alsobeen dependent on the wavelength λ under consideration, but the rest two are not. The only first quantity F_λ gives information about absolute intensity.As a result of (1) we will have intensity distribution $J(x,y)$ in Rayleighs for given wavelength λ. To obtain the calibrated intensity for another wavelength λ we need to have correspondent values F_λ and k_λ.

To obtain the$K_\lambda$values gives absolute value of the light intensity and it we use the LED-based low-light source named as 'PGI-Chernouss-38AM', referred as SID 105 in paper (*Brändström et al.*, 2012). The light source has been additionally tested and equipped by stabilized electric power source. Here we report: i) the results of calibration of two identical cameras from MAIN system, ii) the results of additional testing of the light source SID 105 and its power source.

2. The cameras' calibration

Two identical cameras (named hereinafter as "G-1" and "G-2") used in the MAIN system are based on AVT Guppy F-044B NIR (1/2"CCD) digital cameras which contained type 1/2 (diag. 8 mm) interlaced sensors

SONY CCD ICX429ALL with EXview HAD microlens for enhanced near infrared light sensitivity. However in our case we need to decrease influence of the long-lived oxygen-atom states which gives the auroral red line 630 nm, therefore the cameras have been additionally equipped by blue-green glass filter. The relative responses for the camera sensor and for the glass filter given by manufactures are shown in Fig.1. The optical system includes also an input glass (visually transparent) of the thermal box where the camera is compiled.
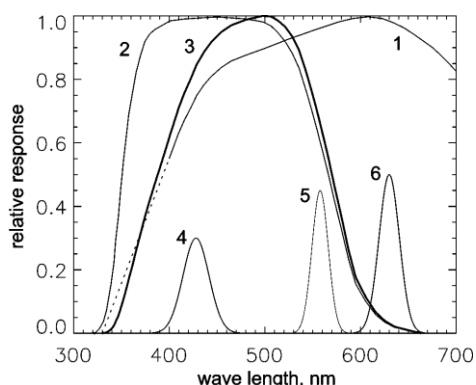
Fig. 1 Relative responses: 1 - SONY CCD ICX429ALL sensor (dotted line – extrapolation in region λ<400 nm); 2 – glass filter C3C21; 3 – $\tau(\lambda)$, theoretical relative response of the optical system (renormalized multiplication of previous two curves); 4, 5, 6 – transmittance of the interference filters.

Relative response of the optical system, $\tau(\lambda)$, estimated by this available information is shown in the Fig.1 by line 3. Three additional filters ('Red', 'Green' and 'Blue') with narrow bandwidths were used for the measurements, their responses are also plotted in Fig.1.

The camera calibrations were provided in optical room of Apatity department of Polar Geophysical Institute during 4 September 2012. The light from the LED-

based light source SID 105 moving through collimator of ~1 m length and through additional interference filter results in a circular patch of 10 pix radius in center of the camera frame. This patch was used as a calibration region and the average intensity over the region was calculated for each frame.

The cameras were operated in Format-7 Mode-2 that gives 376x288 pixels frame. The measurements were repeated 10 times sequentially for 14 gain levels from 0 to 650 with the step 50. Temperature in the camera box was measured continuously and it was equal to 26±1°C. The light source was powered by new set of 3×AA Alcaline batteries for each camera. It was founded that due to different time interval of the measurements (~53 and ~37 minutes) the decrease of the battery voltage was decreased to 15% and 9% for the G1 and G2 cameras, correspondently. Unfortunately, the battery parameters were not measured directly during this session, therefore it was deduced from results of additional measurements described in next section: voltage $V = 4.4\pm0.2$ V and $I_{obs} \approx 380\pm20$ mA.

The "black" field $C_{BF}(x,y)$ was obtained when the light source was tuned off and the input window of the camera was closed. The average "black"(dark current) level in the calibration region, $C_{BF}(x_0,y_0)$, was also calculated from the field for the set of camera gain levels. It was founded that both cameras have individual inhomogeneity of the CCD matrix ('hot pixels') and bright top-left region due to heating of the CCD matrix by other camera components. To obtain the "white" field we used white paper mounted at the wall and illuminated by the low light source from distance ~5 m. To compensate angular inhomogeneity in this case we repeat the measurements with camera rotated at 180° and the results of the measurements was averaged. As a result we found that the matrix $Q(x,y)$ calculated by "black" and "white" fields is practically independent on gain (within <5%), but individual for each camera. The relative difference between the centrum of the $Q(x,y)$ array and in the angles reaches ~50%.
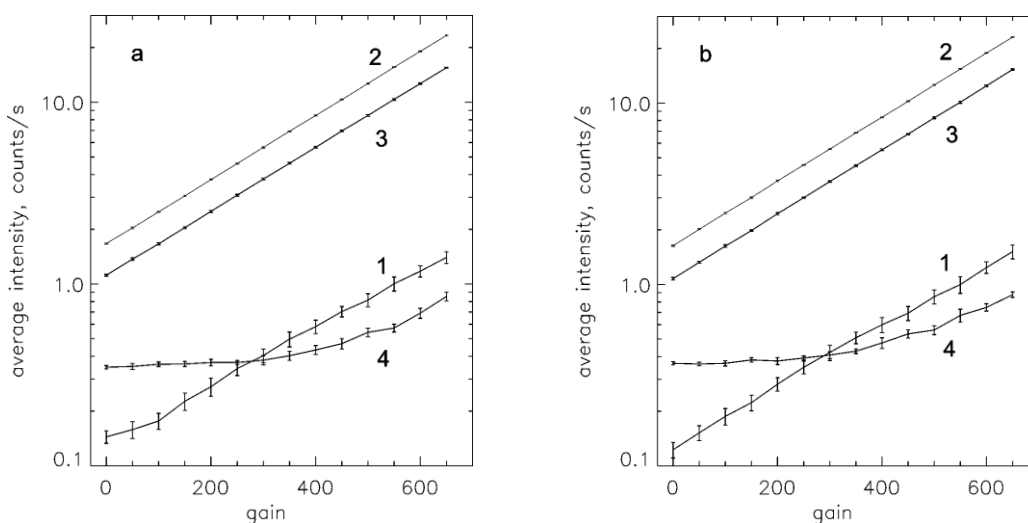
Fig. 2 Average count rate (the light intensity) as a function of the camera gain: a – for camera G-1; b – for camera G-2. Lines 1, 2, and 3 were obtained in correspondent experiments, see Table 2. Line 4 is subtracted background.

The results of the measurements for both cameras are presented in Fig. 2. The lines 1, 2, 3 are the light intensity (in counts per second) registered with 'Red', 'Green' and 'Blue' filters, correspondently, after subtraction of the black level (line 4) obtained for the same region in the CCD matrix. The error bars illustrate the standard deviation of the averaged over the 10 frames value. One can see that the measured curves are perfectly linear in this reference frame, which means the parameterization of the lines is:

$$C_{obs}(g) - C_{BF}(g) = B_\lambda \exp(k_\lambda g), \qquad (3)$$

where B_λ and k_λ are the constants presented in Table 1. For wavelengths of 'Blue' and 'Green' filters the k_λ corresponds well to value ~0.035 dB/step given by manufactors, while for 'Red' filter the value is ~10% less.

Table 1. Parameterization of the lines in Fig. 2 by Eq.(3).

Filter	G-1	G-2
'Red' 630.0 nm	$k_{630.0} = 0.0037$ $B_{630.0} = 0.133$	$k_{630.0} = 0.0038$ $B_{630.0} = 0.123$
'Green' 557.8 nm	$k_{557.8} = 0.00406$ $B_{557.8} = 1.67$	$k_{557.8} = 0.00407$ $B_{557.8} = 1.63$
'Blue' 428.0 nm	$k_{428.0} = 0.00405$ $B_{428.0} = 1.12$	$k_{428.0} = 0.00407$ $B_{428.0} = 1.08$

3. Tests of the light source SID 105

The light source SID 105 was assembled from LED-based flashlight and matt glasses in a tube. The flashlight has 5 intensity settings: 0 – off, 1 – low, 2 – medium, 3 – max, 4 – blinking. During 3 October, 2012 in Apatity we made a set of measurements with the SID 105 powered from several sources. Starting from usual set of batteries we also tested an external laboratory supply with stabilization of voltage. There were two aims for the measurements: i) to follow simultaneously DC current-voltage characteristic of the SID 105 lamp and light intensity during ~30 minutes discharge of new alkaline batteries (the same batteries that was used for measurements by cameras G-1 and G-2 described above); ii) to check proportionality of the light intensity in the selected spectral regions to the DC current through the light source. Then we hope to deduce the correction factors needed due to difference in the DC currents during different calibration experiments.

The measurements with battery power source give us estimations of the battery parameters during camera calibration described in previous section.

Simultaneous measurements of electric and emission parameters of the SID 105 for the intensity settings 1,2 and 3 were performed with stable stationary power source. As a summary of the measurement we can conclude: i) for wavelengths of 'Green' and 'Red' filters the emission efficiency of the LED lamp is nearly constant for all three settings; ii) for 'Blue' filter wavelengths the efficiency increases with lamp current and for setting 3 is even less than for setting 2. The most possible explanation of the last effect is a distortion of the lamp spectrum with current: it is warming at low current. Taking into account a wing of typical very sharp peak at the LED spectrum in the region of 427.8 nm we conclude that the light source cannot be used directly for calibration in this wavelength region. The measured emission efficiencies were normalized by measurements provided in Kiruna on 15 February 2012 and the resulted absolutely calibrated values are presented in Table 2.

Table 2. Efficiency of the SID 105 emission deduced from measurements in Kiruna (15 February 2012).

SID 105 setting	$\varepsilon_{557.3}$ [R mA^{-1}]	$\varepsilon_{629.9}$ [R mA^{-1}]	$\varepsilon_{428.0}$ [R mA^{-1}]
1	33±3	60±13	11.5±0.4
2	58±10	89±16	15.8±0.6
3	67±17	113±45	15.4±0.6

After the study described above we decide to assemble a special stabilized power source with continuous indications of voltage and electric current. We hope this power supply in the future will always be used with the SID 105. The current-voltage characteristics of the SID 105 for intensity settings 1, 2 and 3 measured by this power supply are shown in Fig.3. The error bars are 1% for the voltage and 2% for the current. The experimental points can be inter- and extrapolated by the following empirical dependences:

$$I_{set\_1} = 50\, V_{set\_1} - 90 \qquad (4)$$
$$I_{set\_2} = 300\, (V_{set\_2} - 2.95)^{1/2} + 19 \qquad (5)$$
$$I_{set\_3} = 560\, (V_{set\_3} - 3)^{1/2} + 13 \qquad (6)$$

To apply the results of the light source calibrations to the camera calibration curves we need to deduce the electric circuit parameters used in both cases, and to find a way to renormalized light intensity of the lamp from one case to another.

Taking into account Eq.3, the calibration factor can be found as

$$K_\lambda \left[\text{R s CTS}^{-1} \right] = \frac{\varepsilon_\lambda I_{obs}}{C_{obs}(g) - C_{BF}(g)} = \frac{\varepsilon_\lambda I_{obs}}{B_\lambda} \exp(-k_\lambda\, g) \quad (7)$$

Here for given wavelength λ: ε_λ is calibrated efficiency of the light source (Table 2), I_{obs} is the DC current during camera calibration, B_λ and k_λ – are the camera-dependent constants (Table 1), g is camera gain level.

Comparing with Eq.2, the calibration constant is:

$$F_\lambda\,[\text{R s CTS}^{-1}] = \varepsilon_\lambda I_{obs}\, B_\lambda^{-1} \qquad (8)$$

The results for three wavelengths are shown in Table 3. For $\lambda=427.0$ the calibration factor is increased by factor 1.6 due to trend in the efficiency of the SID 105 emission with electric current (not discussed here in details).

To extrapolate the calibration to other wavelengths we can use known relative spectral response $\tau(\lambda)$, see Fig.1.

153

Taking the $F_{557.7}$ value as a referenced point, we can write:

$$K(\lambda) = \frac{\tau(557.7)}{\tau(\lambda)} K_{557.7} =$$
$$\frac{\tau(557.7)}{\tau(\lambda)} F_{557.7} \exp(-k_{557.7}\, g) \qquad (9)$$

This spectral dependence of the calibration factor is shown in Fig.4 for several camera gain levels. Directly calculated values for λ=557.7 nm, λ=427.0 nm and λ=630.0 nm and gain level g=680 are shown by symbols. While the curves normalized by value for λ=557.7 nm, the directly calculated values for λ=427.0 nm and λ=630.0 nm are also well correspond to the theoretical curve, that is additional validation of the result.
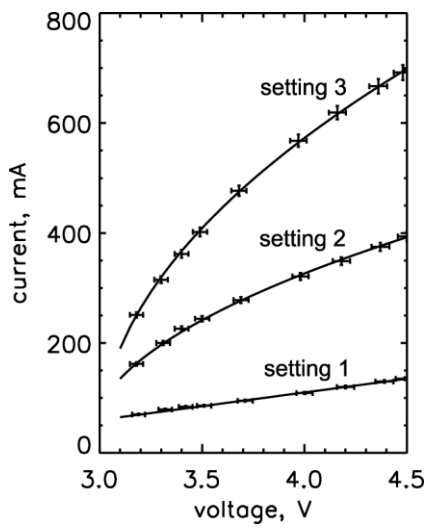
Fig. 3 The current-voltage characteristics of the LED low-light source SID-105 for 3 settings. The crosses are measured points; the lines are the interpolations by equations (4)-(6).

4. Conclusions

Two CCD cameras used for auroral observations (*Kozelov et al.*, 2012) have been calibrated by LED low-light source 'PGI-Chernouss-38AM'. The calibration factor as a function of the wavelength and the camera gain was deduced. Previously the light source PGI-Chernouss-38AM (SID 105) was absolutely calibrated during the intercalibrational workshop of optical low light sources (*Brändström et al.*, 2012), and it was found some issues motivated additional studies of the light source. The current-voltage and emission intensity characteristics of the light source have been measured. It has been found recommendation for the light source users.
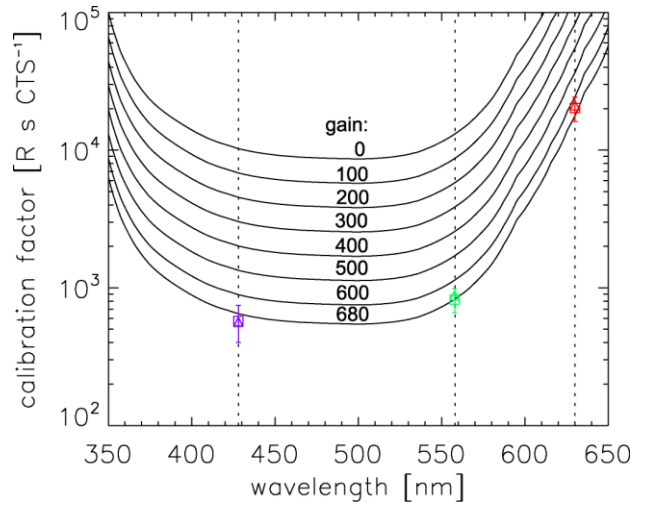
Table 3. Deduced calibration constants for cameras G-1 and G-2 in three wavelengths.

	G-1	G-2
$F_{557.7}$ [R s CTS^{-1}]	1.3×10^4 $\pm 20\%$	1.4×10^4 $\pm 20\%$
$F_{630.0}$ [R s CTS^{-1}]	2.5×10^5 $\pm 20\%$	2.8×10^5 $\pm 20\%$
$F_{427.0}$ [R s CTS^{-1}]	$9 \times 10^{3\,*}$ $\pm 30\%$	$9 \times 10^{3\,*}$ $\pm 30\%$

* increased by factor 1.6.

Fig.4 The G-1 and G-2 cameras calibration factor K_λ. Black lines are the calibration factor for several gain levels. Symbols with error bars are values deduced from calibration by low light source SID 105.

References

Brändström B.U.E., et al.: Results from the intercalibration of optical low light calibration sources 2011, *Geosci. Instrum. Method. Data Syst.*, 1, 43-51, 2012, http://www.geosci-instrum-method-data-syst.net/ 1/43/2012/doi:10.5194/gi-1-43-2012.

Kozelov B.V., et al.: Multi-scale auroral observations in Apatity: winter 2010–2011, *Geosci. Instrum. Method. Data Syst.*, 1, 1–6, 2012, www.geosci-instrum-method-data-syst.net/1/1/2012/doi:10.5194/gi-1-1-2012.

AVT Guppy.*Technical Manual V7.1.0*.Allied Vision Technologies GmbH, Germany. 2009.

154